

# Fast Slow Dynamics - the van der Pol Oscillator

October 2018

# Contents

<b>1 MATLAB Stuff</b>	<b>1</b>
<b>2 Fast-Slow Systems</b>	<b>1</b>
<b>3 Geometric Singular Perturbation Theory</b>	<b>2</b>
<b>4 Singularities and Fold Points</b>	<b>4</b>
<b>5 The Van Der Pol Equation</b>	<b>4</b>
5.1 Derivation of the Van der Pol Fast-Slow System . . . . .	5
5.2 Phase Plane Analysis (is it?? some part 'singularity analysis') . . . . .	6
5.3 Transformation of the Van der Pol System . . . . .	7
5.4 Reduced Dynamics . . . . .	7
5.5 Canonical Form . . . . .	8
5.6 Extended System . . . . .	8
<b>6 The Blow-Up Method</b>	<b>9</b>
6.1 Coordinate Transformation and Charts . . . . .	10
6.2 Dynamics in $K_2$ . . . . .	11
6.3 Dynamics in $K_1$ . . . . .	13
6.4 Dynamics in $K_3$ . . . . .	17
<b>7 Canard Points</b>	<b>17</b>
7.1 Canard Blow-up . . . . .	19
7.1.1 Dynamics in $K_2$ . . . . .	20
7.2 Dynamics in $K_1$ . . . . .	21
7.2.1 Separation of the Manifolds . . . . .	22
7.3 Effect of the Canard Point . . . . .	22
7.3.1 Singular Hopf Bifurcation . . . . .	23
<b>8 Folded Singularities in a Three Dimensional System</b>	<b>23</b>
<b>9 MMO</b>	<b>27</b>
9.1 Oscillations . . . . .	27
9.2 Folded Nodes . . . . .	27
9.3 Singular Hopf Bifurcation . . . . .	27
<b>A Elements of Dynamical Systems</b>	<b>31</b>
A.1 Stable Manifold Theorem . . . . .	31
A.2 Centre Manifold Theorem . . . . .	31
A.3 Implicit Function Theorem . . . . .	31
A.4 Hartman Grobman Theorem . . . . .	31
A.5 Hopf Bifurcations . . . . .	31

<b>B Intuitive Examples</b>	<b>31</b>
B.1 Folded Focus . . . . .	31
<b>C Numerical Simulation</b>	<b>32</b>
<b>D Dynamics in <math>K_2</math></b>	<b>33</b>

## List of Figures

1	Flows in the Van der Pol system.	2
2	Three charts mapping different sections of our blow up (?).	10
3	Phase portrait for chart 2 (?).	11
4	Riccati solution for chart 2 (?).	13
5	Dynamics in chart 1 (?).	14
6	Flow on the Van der Pol system.	17
7	The reduced flow of our system for a) $\lambda = 0$ and b) $\lambda > 0$ .	18
8	The Van der Pol system for the canard case.	19
9	The trajectories associated with the canards case of the Van der Pol system.	22
10	The flow within our canard system (?).	23
11	Three dimensional Van der Pol (?).	24
12	Phase portraits of our three dimensional system where a) is a folded saddle, b) folded node, c) and d) are desingularised flows (?).	26
13	The branches of a spiral	26
14	Oversimplified phase plane for a folded focus.	31

### Abstract

Abstract

## 1 MATLAB Stuff

## 2 Fast-Slow Systems

Fast-Slow systems are systems of differential equations that can be viewed on two different time scales, which are separated by a parameter. These systems are generally of the form

$$\begin{cases} x' = \frac{dx}{dt} = f(x, y, \lambda, \epsilon) \\ y' = \frac{dy}{dt} = \epsilon g(x, y, \lambda, \epsilon), \end{cases} \quad (1)$$

which is called the fast system. Using a change of variables,  $t = \frac{\tau}{\epsilon}$  this can be rewritten as

$$\begin{cases} \epsilon \dot{x} = \epsilon \frac{dx}{d\tau} = f(x, y, \lambda, \epsilon) \\ \dot{y} = \frac{dy}{d\tau} = g(x, y, \lambda, \epsilon), \end{cases} \quad (2)$$

called the slow system.

Here  $x$  is called the fast variable, while  $y$  is the slow variable.  $\lambda$  is a parameter,  $\epsilon$  is the time scale separation parameter and satisfies  $0 < \epsilon \ll 1$ . The functions  $f$  and  $g$  are required to be sufficiently smooth ( depending on literature  $C^1, C^\infty, C^{r+1}$  for  $C^r$  invariant manifolds. Choose later, maybe  $C^r$  considering fenichel theorem) It is generally possible to have three or more time scales, separated by additional time scale separation parameters, as well as more state-space variables.

In order to analyse systems (1) and (2) using Geometric Singular Perturbation Theory (GSPT), the singular limit  $\epsilon \rightarrow 0$  is considered:

$$\begin{cases} x' = \frac{dx}{dt} = f(x, y, \lambda, \epsilon) \\ y' = 0, \end{cases} \quad (3)$$

which is called the layer problem and

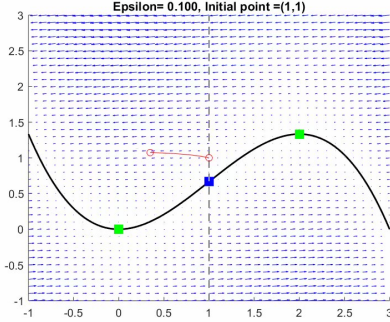
$$\begin{cases} 0 = \epsilon \frac{dx}{d\tau} = f(x, y, \lambda, 0) \\ \dot{y} = \frac{dy}{d\tau} = g(x, y, \lambda, 0), \end{cases} \quad (4)$$

called the reduced system.

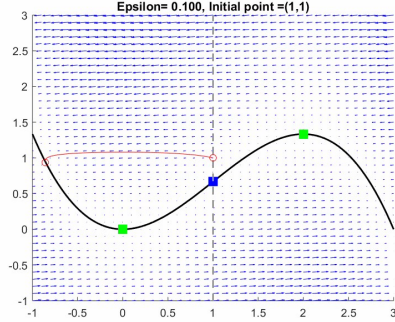
Considering (4), the first equation is  $f(x, y, \lambda, 0) = 0$  and a manifold can be defined as:

$$S = \{(x, y) : f(x, y, \lambda, 0) = 0\}, \quad (5)$$

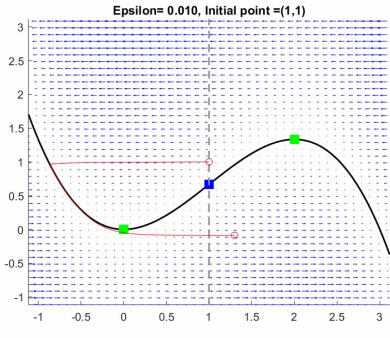
called the critical manifold, where, by definition of  $S$ , the points  $(x, y) \in S$  are equilibria of (3). Before we continue, it is useful to have a visual interpretation of these flows,



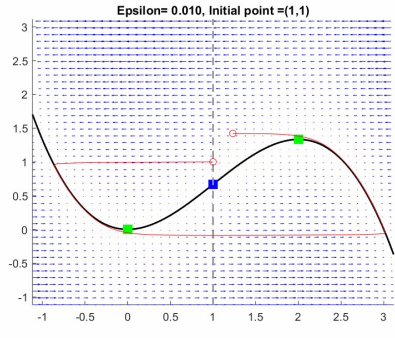
(a) The initial flow within the system starting at  $(x, y) = (1, 1)$ .



(b) The flow as it hits the slow manifold.



(c) The flow as it intersects with the fold point and begins the jump.



(d) The second jump before continuing in a periodic fashion.

Figure 1: Flows in the Van der Pol system.

where we can see that the flows will travel towards our fold point, following the relevant branches. It is worth noting that our flow does not meet the fold point exactly, although this is an ‘error’, it does not directly effect our simulations - as is discussed in Section 1.

### 3 Geometric Singular Perturbation Theory

The main idea of GSPT is the following: Under certain conditions it can be concluded that the critical manifold  $S = S_0$ , where  $\epsilon \rightarrow 0$  persists as an invariant manifold  $S_\epsilon$  under a small perturbation  $\epsilon > 0$ , if  $\epsilon$  is sufficiently small. (In higher than 2 dimensions the idea of transversality of the flow of the stable and unstable manifolds is essential for analysis, while in 2 dimensions this is rather trivial.) The main contribution to GSPT comes from Fenichel Theory and his three Theorems can be summed up in one, according to ( reference MMO Paper or book). However, before stating the Theorem, some formal definitions are needed.

#### Definition 3.1. Normal Hyperbolicity

A submanifold  $M \subseteq S$  is called normally hyperbolic, if the Jacobian  $\frac{\partial f}{\partial x}(x, y, \lambda, 0)$ , where  $(x, y) \in M$ , has only eigenvalues with nonzero real part.

(reference paper 1)

Moreover, the points  $(x, y) \in M$ ,  $M$  normally hyperbolic, are hyperbolic equilibria of (3). (ref:MMO) A normally hyperbolic submanifold can be classified according to its stability property: If  $M$  has only eigenvalues with positive real part it is called repelling, if  $M$  has only eigenvalues with negative real part it is called attracting and if  $M$  is neither attracting nor repelling it is called a saddle-type submanifold. (ref:MMO paper)  
Furthermore, stable and unstable manifolds can be defined as  $W^s(M)$  and  $W^u(M)$ , corresponding to the eigenvalues with negative and positive real part, respectively. (???? pretty sure there are two different concepts in the last two sentences.. check needed) Furthermore, with the following definition it is established which notion of distance is going to be employed throughout this analysis.

### Definition 3.2. Hausdorff Distance

The Hausdorff Distance of two nonempty sets  $V, W \subset \mathbf{R}^n$ , for some  $n \in \mathbf{N}$  is defined as

$$d_H(V, W) = \max\{\sup_{v \in V} \inf_{w \in W} \|v - w\|, \sup_{w \in W} \inf_{v \in V} \|v - w\|\}.$$

(ref: book kuehn)

Now Fenichel's Theorem can be stated:

### Theorem 3.3

#### Fenichel's Theorem

Suppose  $M = M_0$  is a compact, normally hyperbolic submanifold (possibly with boundary) of the critical manifold  $S$  (5) and that  $f, g \in C^r$ ,  $r < \infty$ . Then for  $\epsilon > 0$ , sufficiently small, the following hold:

- (F1) There exists a locally invariant manifold  $M_\epsilon$ , diffeomorphic to  $M_0$ . Local invariance means that  $M_\epsilon$  can have boundaries through which trajectories enter or leave.
- (F2)  $M_\epsilon$  has a Hausdorff distance of  $O(\epsilon)$  from  $M_0$ .
- (F3) The flow on  $M_\epsilon$  converges to the slow flow as  $\epsilon \rightarrow 0$ .
- (F4)  $M_\epsilon$  is  $C^r$ -smooth.
- (F5)  $M_\epsilon$  is normally hyperbolic and has the same stability properties with respect to the fast variables as  $M_0$  (attracting, repelling or saddle type).
- (F6)  $M_\epsilon$  is usually not unique. In regions that remain at a fixed distance from the boundary of  $M_\epsilon$ , all manifolds satisfying (F1)-(F5) lie at a Hausdorff distance  $O(e^{-K/\epsilon})$  from each other for some  $K > 0$  with  $K = O(1)$ .

The normally hyperbolic manifold  $M_0$  has associated local stable and unstable manifolds

$$W^s(M_0) = \cup_{p \in M_0} W^s(p) \quad \text{and} \quad W^u(M_0) = \cup_{p \in M_0} W^u(p),$$

where  $W^s(p)$  and  $W^u(p)$  are the local stable and unstable manifolds of  $p$  as a hyperbolic equilibrium of the layer equations, respectively. These manifolds also persist for  $\epsilon > 0$ , sufficiently small: there exist locally stable and unstable manifolds  $W^s(M_\epsilon)$  and  $W^u(M_\epsilon)$ , respectively, for which conclusions (F1) - (F6) hold if we replace  $M_\epsilon$  and  $M_0$  by  $W^s(M_\epsilon)$  and  $W^s(M_0)$  (or similarly by  $W^u(M_\epsilon)$  and  $W^u(M_0)$ ).

+++direct citation needed for theorem (MMO) +++

Fenichel's Theorem establishes that the submanifold  $M_0$  of the critical manifold  $S_0$  persists as slow manifold  $M_\epsilon$  as  $\epsilon > 0$ , given it is compact and normally hyperbolic. The theorem furthermore establishes that the stable and unstable manifolds persist as well as the individual fibres of these manifolds, namely  $W^s(p)$  and  $W^u(p)$ , that are associated to each base point  $p \in M_0$ . Therefore, under the assumptions of the theorem, the flow of the fast-slow system (1)/(2) remains  $O(\epsilon)$  close to the flow of the system (3)/(4) in the singular limit  $\epsilon \rightarrow 0$ .

The importance of this result lies in the fact that the behaviour of the full system can be analysed by looking at the system in the singular limit instead, which is often more practical.

++++++also trajectories can be constructed and tested using fenichel... paper 1++++++

## 4 Singularities and Fold Points

(ref : book kuehn) One of the requirements of Fenichel's Theorem is normal hyperbolicity. However, fast-slow systems can display singular points where normal hyperbolicity is no longer given and therefore the conclusions of (3.3) no longer hold at these singularities. Singularities in the setting of fast-slow systems are points  $(x_0, y_0)$  on the critical manifold  $S_0$ , for which the Jacobian  $\frac{\partial f}{\partial x}(x_0, y_0, \lambda, 0)$ , has one or more eigenvalues with zero real part. Comparing this with Definition 3.1 shows that this is a negation of normal hyperbolicity. Singularities are points where trajectories can jump between fast and slow flow.

The simplest of those singularities is called a fold point, which is defined as follows:

### Definition 4.1. Fold Point

A fold point  $(x_0, y_0) \in S_0$  is a point where the Jacobian  $\frac{\partial f}{\partial x}(x_0, y_0, \lambda, 0)$  has only one eigenvalue with zero real part.

At the fold point, the system (3) undergoes a saddle-node bifurcation. (+++explain?++++) The fold point is non-degenerate if it satisfies the non-degeneracy assumptions:

$$\begin{cases} \frac{\partial^2 f}{\partial x^2}(x_0, y_0, \lambda, 0) \neq 0 \\ \frac{\partial f}{\partial y}(x_0, y_0, \lambda, 0) \neq 0. \end{cases} \quad (6)$$

Furthermore, if  $(x_0, y_0)$  satisfies the transversality condition  $g(x_0, y_0, \lambda, 0) \neq 0$ , then it is called a generic fold point. For these generic folds there exists a theorem that states that the slow flow on  $S_\epsilon$  (?) near  $(x_0, y_0)$  has either positive or negative sign, implying that no equilibria of the slow flow are close to  $(x_0, y_0)$ . Therefore, for generic fold points no canards will be observed, which is a relevant observation for Section refCanards. The analysis of fold points is using a method called Blow Up Method, which is discussed in Section 6.

In systems containing generic fold point a certain behaviour of the flow can be observed, called Relaxation Oscillations. These are defined as follows:

### Definition 4.2. Relaxation Oscillation

A periodic trajectory  $\gamma_\epsilon$  is the relaxation oscillation of the fast-slow system if the following holds: In the singular limit there exists a trajectory  $\gamma_0$ , which alternates between fast and slow bits and describes a closed loop in the system. This trajectory  $\gamma_0$  persists as  $\gamma_\epsilon$  under a small perturbation  $\epsilon > 0$ .

Systems containing non-generic folds or other types of singularities can display different types of periodic orbits.

## 5 The Van Der Pol Equation

One fast-slow system that contains generic fold points and therefore displays relaxation oscillations is called the Van der Pol System. This can be derived from the Van der Pol Oscillator, which is a well-studied second order ODE that is used to model a variety of physical and biological phenomena. It was developed by the dutch physicist and electrical engineer Balthasar Van der Pol, who conducted research on electrical circuits, in which he observed stable oscillations, later named relaxation oscillations. The derivation of the Van der Pol fast-slow system of the form (1) is presented in the following section.

## 5.1 Derivation of the Van der Pol Fast-Slow System

The Van der Pol Oscillator describes the evolution of the position coordinate  $x(t)$  according to the following the ODE:

$$\ddot{x}(t) - \mu(1 - x^2(t))\dot{x}(t) + x(t) = 0, \quad (7)$$

where  $\mu \gg 1$  is a scalar constant.

A new variable  $w = \dot{x} + \mu F(x)$  is introduced, where  $F(x) = \frac{x^3}{3} - x$ .  $F$  is chosen such that  $F'(x) = -(1 - x^2)$  is the nonlinear term in Equation 7. Differentiating  $w$  we obtain

$$\begin{aligned} \dot{w} &= \ddot{x} + \mu \frac{d}{dx} \left( \frac{x^3}{3} - x \right) \frac{dx}{dt} \\ &= \ddot{x} + \mu(x^2 - 1)\dot{x} \\ &= -x \end{aligned}$$

Here, the last equality follows from rearranging (7). We now have a two dimensional system:

$$\begin{cases} \dot{x} = w - \mu F(x) \\ \dot{w} = -x \end{cases}$$

and letting  $y = \frac{w}{\mu}$  results in

$$\begin{cases} \dot{x} = \mu(y - F(x)) \\ \dot{y} = -\frac{x}{\mu}. \end{cases}$$

Now, using a rescaling of time  $\tilde{t} = \mu\tau$  and setting  $\frac{1}{\mu^2} = \epsilon$  results in the system:

$\dots + \tilde{t}$  is the original variable, we transform into the slow system but state the fast system first because that's the order we always have them in. slightly confusing. ideas? Also. Need to define  $\lambda$  as either zero or 1 depending on where to mention it... $\dots + \dots + \dots + \dots + \dots + \dots$

$$\begin{cases} x' = y - \frac{x^3}{3} + x \\ y' = -\epsilon x, \end{cases} \quad (8)$$

which is of the form (1), the fast system, and the rescaling of time  $t = \epsilon\tau$  results in

$$\begin{cases} \epsilon\dot{x} = y - \frac{x^3}{3} + x \\ \dot{y} = -x, \end{cases} \quad (9)$$

which is in the form of (2), the slow system.

As in Section 2 the fast and slow system can be analysed by considering the limiting case  $\epsilon \rightarrow 0$ . The two systems then become

$$\begin{cases} x' = y - \frac{x^3}{3} + x \\ y' = 0, \end{cases} \quad (10)$$

which is of the form (3), the layer problem, and the reduced problem

$$\begin{cases} 0 = y - \frac{x^3}{3} + x := f \\ \dot{y} = -x. \end{cases} \quad (11)$$

## 5.2 Phase Plane Analysis (is it?? some part 'singularity analysis')

Considering (10), it can be observed that the flow is dominated by the dynamics in  $x$  which is cubically depending on  $x$ . Furthermore, it is clear that in the layer problem the dynamics in  $y$  are constant and therefore the flow is horizontal and is only influenced by  $y$  as a constant parameter. Then  $x$  is called the fast variable. This is immediately obvious when comparing this to the reduced problem (11), where the flow is restricted to  $f = 0$ , which is in the form of a cubic function. This defines a critical manifold. Restricted to this manifold, the flow is dominated by the dynamics in  $y$ , which linearly depends on  $x$ , which is much slower than the cubic dependence in the layer problem. Therefore, this is called the slow flow and  $y$  is the slow variable.

The aim of this analysis is to be able to analyse the system in the singular limit  $\epsilon \rightarrow 0$  and apply appropriate theory to conclude the persistence of the dynamic for  $\epsilon > 0$ . Section 3 introduced one instance where this persistence can be concluded. The main requirement for the theory in Section 3 is normal hyperbolicity of the critical manifold. Considering the manifold  $C_0 = \{(x, y) : 0 = y - \frac{x^3}{3} + x := f\}$ , the Jakobian  $\frac{\partial f}{\partial x}(x, y, 0) = -x^2 + 1$ , which has a zero real part at  $x_0 = \pm 1$ . Together with the corresponding  $y_0$  are singularities of the system. Further analysis has to be done below in order to conclude that they are generic fold points. The points of interest are  $(x_0^+, y_0^+) = (1, -\frac{2}{3})$  and  $(x_0^-, y_0^-) = (-1, \frac{2}{3})$ .

By Definition 4.1, there is only one eigenvalue with zero real part at  $(x_0, y_0)$ . Evaluating the Jakobian at each of the points in turn shows:

$$\begin{cases} \frac{\partial f}{\partial x}(x_0^+, y_0^+, 0) = -1^2 + 1 = 0 \\ \frac{\partial f}{\partial x}(x_0^-, y_0^-, 0) = -(-1)^2 + 1 = 0, \end{cases}$$

where each of the zeros are simple. Therefore  $(x_0^+, y_0^+)$  and  $(x_0^-, y_0^-)$  are fold points. These points are nondegenerate if the non-degeneracy assumptions (6) hold:

$$\begin{cases} \frac{\partial^2 f}{\partial x^2}(x_0^+, y_0^+, \lambda, 0) = -2x_0^+ = -2 \neq 0 \\ \frac{\partial f}{\partial y}(x_0^+, y_0^+, \lambda, 0) = 1 \neq 0, \end{cases}$$

and equivalently for the other fold point

$$\begin{cases} \frac{\partial^2 f}{\partial x^2}(x_0^-, y_0^-, \lambda, 0) = -2x_0^- = 2 \neq 0 \\ \frac{\partial f}{\partial y}(x_0^-, y_0^-, \lambda, 0) = 1 \neq 0. \end{cases}$$

Therefore, the two fold points are non-degenerate. Furthermore, it can be checked if a fold point is generic. It then has to satisfy the transversality condition  $g(x_0, y_0, 0) \neq 0$ . The two fold points considered here are generic, since

$$\begin{aligned} g(x_0^+, y_0^+, 0) &= -1 \neq 0 \\ g(x_0^-, y_0^-, 0) &= 1 \neq 0. \end{aligned}$$

Now we know that the Van der Pol System displays Relaxation Oscillations and that normal hyperbolicity of the system breaks down at the fold points. Fenichel Theory can be applied for regions that are not in the neighbourhood of the fold points. However, a different approach has to be employed for the analysis of the dynamics around the folds.

In order to analyse a fold point it is convenient to transform the Van der Pol system using a coordinate transformation that satisfies the following:

$$\begin{cases} (x_0, y_0) = (0, 0) \text{ is a fold point,} \\ \frac{\partial^2 f}{\partial x^2}(0, 0, 0) > 0 \\ \frac{\partial f}{\partial y}(0, 0, 0) < 0 \\ g(0, 0, 0) < 0. \end{cases} \quad (12)$$

### 5.3 Transformation of the Van der Pol System

In order to analyse the system at the fold points, one fold point at  $(x_0^+, y_0^+) = (1, -\frac{2}{3})$  is considered, and the further analysis is identical for the second fold point  $(x_0^-, y_0^-)$  with a slightly different coordinate transformation. The aim is to find a coordinate transformation that satisfies the conditions in (12). The proposed transformation is  $(x, y) \rightarrow (1 - \tilde{x}, \tilde{y} - \frac{2}{3})$ , which represents a reflection and a translation of the system such that  $(x_0^+, y_0^+)$  is mapped to  $(0, 0)$  - Figure ??.

Now using the proposed mapping  $(x, y) \rightarrow (1 - \tilde{x}, \tilde{y} - \frac{2}{3})$  we are able to redefine the fast system (8) in the following way,

$$\begin{cases} x' = -y + x^2 - \frac{(x)^3}{3} \\ y' = \epsilon(x - 1), \end{cases} \quad (13)$$

where the tilde has been dropped on  $x$  and  $y$  for convenience. The slow system (9) is redefined as

$$\begin{cases} \epsilon x' = -y + x^2 - \frac{(x)^3}{3} \\ y' = (x - 1), \end{cases} \quad (14)$$

using the normal rescaling of time. These two systems will be used throughout the following analysis of the generic fold point. We should note that we have used the general system (Equations 1) to produce the new system where we have chosen  $\lambda = 1$ .

It is readily checked that the coordinate transformation is correct by evaluating (12) for the transformed system. It is clear to see that  $(x_0, y_0) = (0, 0)$ , and differentiation of  $f$  yields  $\frac{\partial^2 f}{\partial x^2}(0, 0, 0) = 2 > 0$  and  $\frac{\partial^1 f}{\partial y^1}(0, 0, 0) = -1 < 0$ . Furthermore,  $g(0, 0, 0) = -1 < 0$ . Therefore, the new system of equations possesses the required qualities.

### 5.4 Reduced Dynamics

In order to determine the reduced dynamics on the critical manifold  $S$ , Equation 14 in the limit  $\epsilon \rightarrow 0$  is considered which yields the following system,

$$\begin{cases} 0 = f(x, y, 0) = -y + x^2 - \frac{x^3}{3} \\ \dot{y} = g(x, y, 0) = 0 \end{cases} \quad (15)$$

which is the reduced problem (?). The critical manifold is then defined as

$$S = \{(x, y) : f(x, y, 0) = 0\} = \left\{ (x, y) : y = x^2 - \frac{x^3}{3} \right\}, \quad (16)$$

which is an S-shaped curve. Since the flow on  $S$  is determined by  $\dot{y}$ , it can be seen that since the sign of  $g$  is negative in the neighbourhood of the fold point  $(0, 0)$ , the slow flow on  $S$  is directed towards the fold point.

The two fold points  $(x_0^\pm, y_0^\pm)$  coincide with the extrema of the cubic function  $\phi(x) = y = x^2 - \frac{x^3}{3}$ . Then using the chain rule, the second Equation of 15 is (?),

$$\phi_x(x)\dot{x} = g(x, \phi(x), 0). \quad (17)$$

Rearranging this gives an expression for the dynamics in  $x$  on  $S$ . We find that  $\phi(x) = x^2 - \frac{x^3}{3}$ , where the derivative with respect to  $x$  gives  $\phi_x(x) = 2x - x^2$ . Therefore (17) becomes

$$\dot{x} = \frac{g(x, \phi(x), 0)}{\phi_x(x)} = \frac{x-1}{2x-x^2} = \frac{x-1}{x(2-x)}.$$

This calculation confirms that the fold points at  $x = 0$  and  $x = 2$  are singularities of the reduced system. Therefore, no conclusions about the dynamics of  $x$  can be made at the fold points. Different methods will have to be developed in order to overcome this.

## 5.5 Canonical Form

In order to simplify the analysis below, it is useful to rewrite the dynamical system in canonical form.

$$\begin{aligned} x' &= -y + x^2 - \frac{x^3}{3} = -y + x^2 + h(x) \\ y' &= \epsilon(x-1) \end{aligned} \quad (18)$$

There is ample reasoning for doing this. The canonical form has been studied in great detail, allowing us to make comparisons and to avoid excess computation, as seen in ? paper on Extending Geometric Singular Perturbation Theory. Note that the first equation has, locally, the shape of the parabola  $y = x^2$ , which reflects the consideration of the fold point  $(0, 0)$ , which is locally the minimum of a parabola.

## 5.6 Extended System

The canonical system (18) is then extended to three dimensions by considering  $\epsilon' = 0$ .

$$\begin{aligned} x' &= -y + x^2 + h(x) \\ y' &= \epsilon(x-1) \\ \epsilon' &= 0. \end{aligned} \quad (19)$$

Analysing the stability of the three dimensional system, three eigenvalues can be found by considering the Jacobian matrix, in the singular limit  $\epsilon = 0$ :

$$J = \begin{vmatrix} 2x-x^2 & -1 & 0 \\ 0 & 0 & 0 \\ 0 & 0 & 0 \end{vmatrix} \quad (20)$$

This is an upper triangular matrix and hence  $(\lambda_1, \lambda_2, \lambda_3) = \text{tr}(J) = (2x-x^2, 0, 0)$ . Therefore, at the fold points, where  $x = 0$  or  $x = 2$ ,  $\lambda_i = 0$  for  $i = 1, 2, 3$ . Therefore, there exists a zero eigenvalue on  $S$  at the fold points. At these points  $S$  is not normally hyperbolic. The critical manifold has to be divided as follows:

$$\begin{aligned} S^a &= \{(x, y) : y = x^2 - \frac{x^3}{3}, x < 0\} \cup \{(x, y) : y = x^2 - \frac{x^3}{3}, x > 2\} \\ S^r &= \{(x, y) : y = x^2 - \frac{x^3}{3}, 0 < x < 2\}, \end{aligned}$$

such that  $S^a \cup S^r \cup \{0\} \cup \{2\} = S$ . The manifolds  $S_0^a$  and  $S_0^r$  are normally hyperbolic everywhere and Fenichel's Theorem (3.3) can be applied in order to conclude the persistence of the manifold as slow manifolds  $S_\epsilon^a$  and  $S_\epsilon^r$ . At the points  $\{0\}$  and  $\{2\}$  the normal hyperbolicity is not given, since the eigenvalue associated to  $S$  is zero at these points. ++++++Note: technically the paper mentions here the centre manifold  $M$ , stressing the three dimensionality of the problem. if we want that it can be added++++++

The problem that the Van der Pol System provides now is the analysis at the fold points. In the analysis of the reduced system it became apparent that the fold points are singularities of the reduced flow on  $S_0$ , and therefore the dynamics in the singular limit cannot be determined. Furthermore, Fenichel Theory does not apply at the folds because normal hyperbolicity breaks down at these points, as discussed above. Therefore, even if the dynamics around the folds in the singular limit was known, no conclusions could be drawn for the perturbed system with  $S_\epsilon$ . Alternative methods have to be employed to describe the dynamics on the fold points in the singular limit and furthermore to be able to conclude the dynamics of the full system at the fold points from this analysis. The method considered for analysis is called the Blow-Up Method and is considered in the following section.

## 6 The Blow-Up Method

+++Rename chapter: 'The Blow-Up Method'++++++

In order to apply the Blow-Up Method to the fold point at the origin, we focus on a neighbourhood  $U$  around the fold point  $(0, 0)$ . The neighbourhood  $U$  is small enough, such that  $g(x, y, \epsilon) \neq 0$  in  $U$ , and we can define sections in  $U$ , as follows:

$$\begin{aligned}\Delta^{in} &= \{(x, \rho^2), x \in I\} \\ \Delta^{out} &= \{(\rho, y), y \in \mathbf{R}\},\end{aligned}$$

where  $I \subset \mathbf{R}$ . Now  $\Delta^{in}$  is traverse to  $S^a$ , while  $\Delta^{out}$  is traverse to the fast flow. This enables us to monitor the incoming trajectories from the attracting branch of  $S$  and the trajectories leaving  $U$  in the direction of the fast flow. Then a function  $\pi : \Delta^{in} \rightarrow \Delta^{out}$  can be defined, called the transition map, which describes how the trajectories passing through  $\Delta^{in}$  are mapped onto the outgoing flow in  $\Delta^{out}$ . The following theorem describes the behaviour of the flow under  $\pi$  and a sketch of the proof will be given at the end of this section: +++last statement not precise+++

### Theorem 6.1 (?)

*Under the assumptions made in this section, there exists  $\epsilon_0 > 0$  such that the following assertions hold for  $\epsilon \in (0, \epsilon_0]$ :*

1. *The manifold  $S_\epsilon^a$  passes through  $\Delta^{out}$  at a point  $(\rho, h(\epsilon))$ , where  $h(\epsilon) = O(\epsilon^{2/3})$ .*
2. *The transition map  $\pi$  is a contraction with contraction rate  $O(e^{-c/\epsilon})$ , where  $c$  is a positive constant.*

This means that the trajectories that enter  $U$  through  $\Delta^{in}$ , will be funneled into a smaller section of  $\Delta^{out}$  and therefore we are guaranteed to observe the trajectories that enter through  $\Delta^{in}$  in  $\Delta^{out}$ .

Now we are in the position to describe the Method of Blow-Up Transformations in the neighbourhood  $U$ .

## 6.1 Coordinate Transformation and Charts

We first need to transform the extended system (19) with respect to the time variable and the space variables. This coordinate transformation is called the Blow-Up Transformation because the degenerate fold point  $(0, 0)$  (eigenvalue 0, refer to extended system) is regarded as a sphere of radius  $r = 0$ . By rescaling the space variables with respect to different weights of  $r$ ,

$$x = \bar{r}\bar{x} \quad (21a)$$

$$y = \bar{r}^2\bar{y} \quad (21b)$$

$$\epsilon = \bar{r}^3\bar{\epsilon}, \quad (21c)$$

we find that we are able to carry out further analysis, as will follow. +++++ If time and space permit, an analysis of the space  $B$  and coordinate map would be good... p.291 krupa++++ Instead of analysing the sphere in polar coordinates, which might seem the most obvious choice of method, the rest of this analysis is done using charts, which are introduced in the next section. This method turns out to be a more natural choice for this problem and maximises computational efficiency. In terms of the blown up fold point, a sphere denoted by

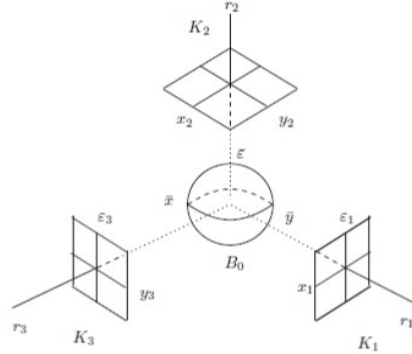


Figure 2: Three charts mapping different sections of our blow up (?).

$B$ , charts are projections of regions of  $B$  onto a two dimensional plane. We introduce three charts  $K_1, K_2$ , and  $K_3$ . Chart  $K_2$  is the two dimensional projection covering the upper half plane of  $B$ . However, as points on the equator of  $B$  are approached on  $K_1$ , we tend to infinity. These regions however, are of immense interest, since they are points of incoming and outgoing trajectories. As a consequence, charts  $K_1$  and  $K_3$  are introduced, covering the regions of interest on the equator of the fold point. These charts will be discussed in detail in the sections to follow.

The charts are defined by setting each of the variables of the extended system to 1 in turn, giving  $\bar{y} = 1$ ,  $\bar{\epsilon} = 1$ ,  $\bar{x} = 1$ . Substituting these into Equations (21a), (21b) and (21c) respectively gives,

$$x = r_1 x_1, \quad y = r_1^2, \quad \epsilon = r_1^3 \epsilon_1, \quad (22a)$$

$$x = r_2 x_2, \quad y = r_2^2 y_2, \quad \epsilon = r_2^3 \epsilon_2 \quad (22b)$$

$$x = r_3, \quad y = r_3^2 y_3, \quad \epsilon = r_3^3 \epsilon_3 \quad (22c)$$

where  $(x_i, r_i, \epsilon_i) \in \mathbf{R}^3$  for  $i = 1, 2, 3$ , and the equations correspond to the charts in numerical order (?). With this setup, we can consider the individual charts in turn, analyse the dynamics on the individual charts, and then join the gathered information into a global view on the dynamics in  $U$ . We start with  $K_2$ , because it holds

the most information and the flow is analysed more readily than in the other two charts. The remaining question is how the transition between the three charts and the connection to the global dynamics is made after finishing the individual analysis. This is done via a coordinate change, derived by using equations (22) and (21), and the results are summed up in the following Lemma:

### Lemma

Let  $\kappa_{12}$  denote the change of coordinates from  $K_1$  to  $K_2$ . Then  $\kappa_{12}$  is given by

$$x_2 = x_1 \epsilon_1^{-1/3}, y_2 = \epsilon_1^{-2/3}, r_2 = r_1 \epsilon_1^{1/3}, \quad (23)$$

for  $\epsilon_1 > 0$ , and  $\kappa_{12}^{-1}$  is given by

$$x_1 = x_2 y_2^{-1/2}, r_1 = r_2 y_2^{1/2}, \epsilon_1 = y_2^{-3/2}, \quad (24)$$

for  $y_2 > 0$ . Let  $\kappa_{23}$  denote the change of coordinates from  $K_2$  to  $K_3$ . Then  $\kappa_{23}$  is given by

$$r_3 = r_2 x_2, y_3 = y_2 x_2^{-2}, \epsilon_3 = x_2^{-3}, \quad (25)$$

for  $x_2 > 0$ , and  $\kappa_{23}^{-1}$  is given by

$$x_2 = \epsilon_3^{-1/3}, y_2 = y_3 \epsilon_3^{-2/3}, r_2 = r_3 \epsilon_3^{1/3}, \quad (26)$$

for  $\epsilon_3 > 0$ .

Furthermore, transition maps  $\Pi_i, i \in 1, 2, 3$  are defined in each section, describing how the trajectories coming in and out of each chart. These are combined in the final part of this section to give the proof of Theorem 6.1, and to relate the results of the blow up method back to the original transition map  $\pi$ .

## 6.2 Dynamics in $K_2$

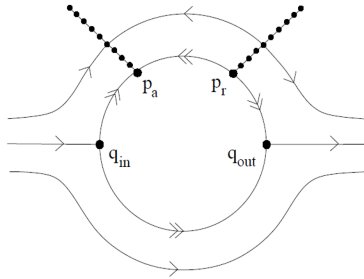


Figure 3: Phase portrait for chart 2 (?).

To be able to consider chart  $K_2$ , the transformation presented in Equation (22b) is applied to the extended system (19). Furthermore, a time rescaling ( $t_2 = r_2 t$ ) is applied to desingularise the system. This results in:

$$\frac{d}{dt}(r_2 x_2) = r_2^2 \frac{dx_2}{dt} = -y_2 + x_2^2 - \frac{x_2^3 r_2}{3}, \quad (27)$$

$$r_2^3 y'_2 = r_2^3 (-1 + r_2 x_2), \quad (28)$$

$$r'_2 = 0, \quad (29)$$

noting that  $\frac{dr}{dt_2} = \frac{dt}{dt_2} \frac{dr}{dt} = \frac{1}{r_2} \frac{dr_2}{dt}$ . Now dividing through by  $r_2^2$  and  $r_2^3$  respectively for each equation and grouping  $O(r_2)$  terms we get,

$$\begin{aligned} x'_2 &= x_2^2 - y_2 + O(r_2), \\ y'_2 &= -1 + O(r_2), \\ r'_2 &= 0. \end{aligned} \tag{30}$$

Then, considering  $r_2 = 0$  and neglecting the  $O(r_2)$  terms results in:

$$\begin{aligned} x'_2 &= x_2^2 - y_2, \\ y'_2 &= -1, \end{aligned} \tag{31}$$

which are the well known Riccati equations- see ?. Some known results about the Riccati equations can be summarised as follows:

**Proposition 6.2 (?)**

*The Riccati equation (31) has the following properties:*

1. Every orbit has a horizontal asymptote  $y = y_r$ , where  $y_r$  depends on the orbit such that  $x \rightarrow \infty$  as  $y$  approaches  $y_r$  from above.
2. There exists a unique orbit  $\gamma_2$ , which can be parameterized as  $(x, s(x))$ ,  $x \in \mathbf{R}$  and is asymptotic to the left branch of the parabola  $x^2 - y = 0$ , for  $x \rightarrow -\infty$ . The orbit  $\gamma_2$  has a horizontal asymptote  $y = -\Omega_0 < 0$ , such that  $x \rightarrow \infty$  as  $y$  approaches  $-\Omega_0$  from above.
3. The function  $s(x)$  has the asymptotic expansions

$$\begin{aligned} s(x) &= x^2 + \frac{1}{2x} + O\left(\frac{1}{x^4}\right), x \rightarrow -\infty, \\ s(x) &= -\Omega_0 + \frac{1}{x} + O\left(\frac{1}{x^3}\right), x \rightarrow \infty. \end{aligned}$$

4. All orbits to the right of  $\gamma_2$  are backward asymptotic to the right branch of the parabola  $x^2 - y = 0$ .
5. All orbits to the left of  $\gamma_2$  have a horizontal asymptote  $y = y_l > y_r$ , where  $y_l$  depends on the orbit, such that  $x \rightarrow -\infty$  as  $y$  approaches  $y_l$  from below.

The solutions to the Riccati equations, described in Proposition 6.2, are displayed in Figure. Note that the equation  $x^2 - y = 0$  is locally the critical manifold  $S$  close to the fold point, under neglegation of  $r_2$  terms.++a bit wavy argument++ The orbit  $\gamma_2$ , corresponds to the global trajectory  $\gamma$ , of the full system, which is the candidate trajectory connecting the slow flow on  $S^a$  entering  $U$  through  $p_a$  to the fast fibres, exiting  $U$  through  $q_{out}$  - described by Figure 4.

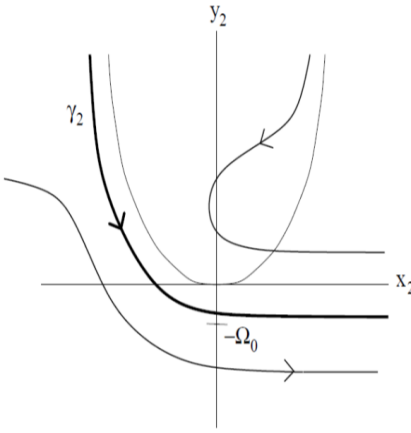


Figure 4: Riccati solution for chart 2 (?).

This leads to the conclusion that if we can connect  $\gamma_2$  to  $p_a$  through  $K_1$  and to  $q_{out}$  through  $K_3$ , the global  $\gamma$  can be constructed using Lemma 6.1. This motivates the analysis of  $K_1$  and  $K_3$ . In order to connect the dynamics on  $K_2$  to that on the other charts, we need to define local inflow and outflow sections, similar to  $\Delta^{in}$  and  $\Delta^{out}$  in the full system. Then we can follow trajectories that get mapped by  $\Pi_2$ , again analogous to  $\pi$  in the full system, from a section  $\Sigma_2^{in}$  to  $\Sigma_2^{out}$ . The section are defined as follows. For  $\delta > 0$ , we have:

$$\begin{aligned}\Sigma_2^{in} &= \{(x_2, y_2, r_2) : y_2 = \delta^{-2/3}\}, \\ \Sigma_2^{out} &= \{(x_2, y_2, r_2) : x_2 = \delta^{-1/3}\}.\end{aligned}$$

Then the transition map  $\Pi_2$  can be defined and the results are summarised as follows:

### Proposition 6.3 (?)

*The transition map  $\Pi_2$  has the following properties:*

1.

$$\Pi_2(q_0) = (\delta^{-1/3}, -\Omega_0 + \delta^{1/3} + O(\delta), 0)$$

2. *A neighbourhood of  $q_0$  is mapped diffeomorphically onto a neighbourhood of  $\Pi_2(q_0)$ .*

This is sufficient information to now consider the dynamics on  $K_1$ .

### 6.3 Dynamics in $K_1$

The coordinate transformation (22a) is applied to the extended system (19), and a rescaling of time ,  $t_1 = r_1 t$ , to get

$$\begin{aligned}\frac{d(r_1 x_1)}{dt_1} \frac{dt_1}{dt} &= -r_1^2 + r_1^2 x_1^2 - \frac{1}{3} r_1^3 x_1^3 \\ \frac{dr_1^2}{dt_1} \frac{dt_1}{dt} &= 2r_1^2 r_1' = r_1^3 \epsilon_1 (-1 + r_1 x_1) \\ \frac{d(r_1^3 \epsilon_1)}{dt_1} \frac{dt_1}{dt} &= (3r_1^2 \epsilon_1 + r_1^3 \epsilon_1') r_1 = 0.\end{aligned}$$

Dividing through by  $\frac{dt_1}{dt} = r_1$  and replacing the expressions for  $\epsilon'_1$  and  $r'_1$  with their expressions in terms of the variables, results in the full system in terms of  $K_1$ . Note that the equation for  $\epsilon'$  is found by rearranging the third equation above.

$$\begin{aligned}x'_1 &= -1 + x^2 + \frac{1}{2}x_1\epsilon_1 + \left( -\frac{1}{2}\epsilon_1x_1^2r_1 - \frac{1}{3}x_1^3 \right) \\r'_1 &= \frac{1}{2}r_1\epsilon_1(-1 + r_1x_1) \\\epsilon'_1 &= \frac{3}{2}\epsilon_1^2(1 - r_1x_1),\end{aligned}$$

and grouping terms in  $r_1$  results in the standard form:

$$x'_1 = -1 + x^2 + \frac{1}{2}x_1\epsilon_1 + O(r_1) \quad (32)$$

$$r'_1 = \frac{1}{2}r_1\epsilon_1(-1 + O(r_1)) \quad (33)$$

$$\epsilon'_1 = \frac{3}{2}\epsilon_1^2(1 - O(r_1)). \quad (34)$$

The system (32) has two invariant planes, that are somewhat equivalent to the notion of a nullcline. In an invariant plane, one of the parameters do not change their value and here these are  $r_1 = 0$  and  $\epsilon_1 = 0$ . If we substitute  $r_1 = 0$  or  $\epsilon_1 = 0$  into (32), the  $r_1$  equation, or  $\epsilon_1$  equation respectively, vanishes, and there is only a two dimensional system left to consider. These two subspaces of (32) will be analysed below. Furthermore, the subspace where  $r_1 = 0$  and  $\epsilon_1 = 0$ , is one dimensional, an invariant line, where the subspaces  $r_1 = 0$  and  $\epsilon_1 = 0$  cross. The following analysis is displayed in Figure 5, illustrating the dynamics on  $K_1$ .

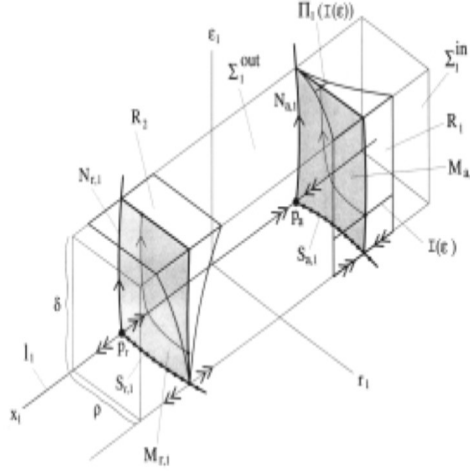


Figure 5: Dynamics in chart 1 (?)

The invariant line, satisfying  $r_1 = 0$  and  $\epsilon_1 = 0$  is given by  $l_1 = -1 + x^2$ . From this it is easily deduced that the two equilibrium points are where  $l_1 = 0$ , which is at  $x = \pm 1$ . Therefore, the points  $p_a$  and  $p_r$  are defined as  $p_a = (-1, 0, 0)$  and  $p_r = (1, 0, 0)$ . The flow on  $l_1$  is attracted to  $p^a$  and repelled by  $p^r$ , which is easily observed from the form  $l_1$  takes or from a formal stability analysis of the one dimensional system. The eigenvalues of  $l_1$  are found by considering  $l'_1 - \lambda = 2x - \lambda = 0$  which gives that  $\lambda = \pm 2$  at the respective equilibria.

Then we expect the behaviour of the flow on the two invariant planes to be influenced by the two equilibria and the dynamics on  $l_1$ . Consider the plane  $\epsilon_1 = 0$ . The system (32) becomes

$$x'_1 = -1 + x^2 - \left( \frac{1}{3} r_1 x_1^3 \right) \quad (35)$$

$$r'_1 = 0. \quad (36)$$

This system has equilibria at  $x = \pm 1$ , for  $r_1 = 0$ , as before, however, for each constant value of  $r_1$ , we get a different equilibrium of the system (35). This forms a curve of equilibria, which can be recognise as  $S_1^a$  connected to  $p_a$  and  $S_1^r$ , connected to  $p_r$ , the left and right branches of the critical manifold, transformed into  $K_1$ . This is well illustrated in figure 3. Note. apparently this follows from IFT we got stuck on this before, i cannot remember :(+++++++++) The additional eigenvalue, corresponding to the  $r_1$  equation, is  $\lambda = 0$ . However, at each of the equilibria of this system, and specifically at  $p_a$  and  $p_r$  we have normal hyperbolicity, due to the coordinate transformation in  $K_1$ . ++ go over this. +++

Next we consider the dynamics on the invariant plane  $r_1 = 0$ . The system (32) becomes:

$$x'_1 = -1 + x^2 + \frac{1}{2} x_1 \epsilon_1 \quad (37)$$

$$\epsilon'_1 = \frac{3}{2} \epsilon_1^2. \quad (38)$$

Again,  $x = \pm 1$  are equilibria of the system, and an additional zero eigenvalue is gained due to the  $\epsilon$  equation. It can be concluded that one dimensional centre manifolds exist, called  $N_{a,1}$  and  $N_{r,1}$ , that are invariant, however, not manifolds of equilibria like  $S^a$  and  $S^r$  in the  $\epsilon = 0$  plane. The dynamics on these manifolds is determined mainly by the value of  $\epsilon$ , since the change in the  $\epsilon$  direction is much stronger than the change in the  $x$  direction. Therefore, on  $N_{a,1}$  and  $N_{r,1}$  the flow moves up the  $\epsilon$  direction with increasing epsilon.

In order to draw conclusions on the persistence of the dynamics in the full system (+++??+++) **What does this mean?**, as before, sections in the space are defined to monitor incoming and outgoing trajectories. Firstly, let the region considered be such that  $D_1 := \{(x_1, y_1, \epsilon_1) : x_1 \in \mathbf{R}, 0 \leq r_1 \leq \rho, 0 \leq \epsilon_1 \leq \delta\}$ . Then the relevant sections for the candidate trajectory  $\gamma$  are

$$\begin{aligned} \Sigma_1^{in} &:= \{(x_1, r_1, \epsilon_1) \in D_1 : r_1 = \rho\}, \\ \Sigma_1^{out} &:= \{(x_1, r_1, \epsilon_1) \in D_1 : \epsilon_1 = \delta\}. \end{aligned}$$

Note that  $\Sigma_1^{in} = \Delta^{in}$  and  $\Sigma_1^{out} = \Sigma_2^{in}$ . The aim is to find the connection between  $p_a$  and  $\gamma_2$  in  $K_2$ . In order to establish this connection, the trajectory  $\gamma_2$  has to be mapped onto  $K_1$  using Lemma 6.1. Recall from Section 6.2 that the form of the candidate trajectory is of the form  $(x_2, s(x_2))$ . Therefore, the trajectory  $\gamma_1$  satisfies:

$$(x_1, 0, \epsilon_1) = \left( x_2 \left( x_2^2 + \frac{1}{2x_2} + O\left(\frac{1}{x_2^4}\right) \right)^{-1/2}, 0, \left( x_2^2 + \frac{1}{2x_2} + O\left(\frac{1}{x_2^4}\right) \right)^{-3/2} \right).$$

Note that  $s(x_2)$  as  $x_2 \rightarrow -\infty$  is employed, since we consider the left continuation of  $\gamma_2$ . Furthermore, as is intuitively clear from Figure 4, and can be shown by analysing the form of  $\gamma_1$ , the trajectory  $\gamma_1$  converges to

$p_a$  in backward time, which is exactly as expected. This establishes the link between the slow flow on  $S^a$  and the flow on  $K_2$ , if we consider the following proposition, which sums up the findings in  $K_1$  and employs center manifold theory, see Appendix (++++how do i reference that?++++) in order to establish persistence in the full system.

**Proposition 6.4 (?)**

For  $\rho, \delta$  sufficiently small the following assertions hold for the system 32:

1. There exists an attracting two-dimensional  $C^k$ -center manifold  $M_{a,1}$  at  $p_a$  which contains the line of equilibria  $S_1^a$  and the center manifold  $N_{a,1}$ . In  $D_1$  the manifold  $M_{a,1}$  is given as a graph  $x_1 = h_a(r_1, \epsilon_1)$ . The branch of  $N_{a,1}$  in  $r_1 = 0, \epsilon_1 > 0$  is unique.
2. There exists a repelling two-dimensional  $C^k$ -center manifold  $M_{r,1}$  at  $p_r$  which contains the line of equilibria  $S_1^r$  and the center manifold  $N_{r,1}$ . In  $D_1$  the manifold  $M_{r,1}$  is given as a graph  $x_1 = h_r(r_1, \epsilon_1)$ . The branch of  $N_{r,1}$  in  $r_1 = 0, \epsilon_1 > 0$  is not unique.
3. There exists a stable invariant foliation  $F^s$  which base  $M_{a,1}$  and one-dimensional fibres. For any  $c > -2$  there exists a choice of positive  $\rho$  and  $\delta$  such that the contraction along  $F^s$  during a time interval  $[0, T]$  is stronger than  $e^{cT}$ .
4. There exists an unstable invariant foliation  $F^u$  which base  $M_{r,1}$  and one-dimensional fibres. For any  $c > -2$  there exists a choice of positive  $\rho$  and  $\delta$  such that the expansion along  $F^u$  during a time interval  $[0, T]$  is stronger than  $e^{cT}$ .
5. The unique branch  $N_{a,1}$  in  $r_1 = 0, \epsilon_1 > 0$  is equal to  $\gamma_1 := \kappa_{12}^{-1}(\gamma_2)$  wherever  $\kappa_{12}^{-1}(\gamma_2)$  is defined, i.e. along the part of  $\gamma_2$  corresponding to  $y_2 > 0$ .

In order to find the lower bound on the contraction rate along  $F^s$ , the transition time  $T$  has to be found, i.e. the time the trajectory takes to travel from a point  $p = (x_1, \rho, \epsilon_1) \in \Sigma_1^{in}$  to a point in  $\Pi_1(p) = (x_1, r_1, \delta) \in \Sigma_1^{out}$ . This is done by integrating the  $\epsilon$  equation of system (32), which is a separable ODE with respect to  $t_1$ . This then results in

$$T = \frac{2}{3} \left( \frac{1}{\epsilon_1} - \frac{1}{\delta} \right) (1 + O(\rho)),$$

where  $r_1 = \rho \in p$ . Therefore, a transition map  $\Pi_1 : \Sigma_1^{in} \rightarrow \Sigma_1^{out}$  can be defined for small enough parameter values of  $\rho, \delta, \beta_1$  (Why only for small param.?++++++). We are interested specifically in the transition around the center manifolds  $M_{a,1}$  and  $M_{r,1}$ . The following subsections of  $\Sigma_1^{in}$  and  $\Sigma_1^{out}$  can be defined. Let  $R_1 = \{(x_1, \rho, \epsilon_1) : |1 + x_1| \leq \beta_1\}$ , a rectangle in the intersection of the manifolds  $M_{a,1}$  and  $\Sigma_1^{in}$ , and  $R_2 = \{(x_1, r_1, \delta) : |1 - x_1| \leq \beta_1\}$ , a rectangle in the intersection of the manifolds  $M_{r,1}$  and  $\Sigma_1^{out}$ , with  $\beta_1 > 0$  sufficiently small. Furthermore, we can define line segments in these rectangles as  $I_a(\bar{\epsilon}) \subset R_1$  and  $I_r(\bar{r}) \subset R_2$ , where  $0 \leq \bar{\epsilon} \leq \delta$  and  $0 \leq \bar{r} \leq \rho$ . Then for any  $\bar{\epsilon}$ ,  $\Pi_1$  maps the trajectory on a smaller region  $\Pi_1 I_a(\bar{\epsilon}) \in \Sigma_1^{out}$ . This is called a contraction of the trajectories. Considering Theorem 6.1, which states the dependence of the contraction rate on  $\epsilon$ , the bounds on the contraction rate can be related to  $\epsilon$ , the parameter of the original system. Then using the  $K_1$  rescaling of  $\epsilon = \epsilon_1 r_1^3$ , see (22a), the contraction rate for  $\Pi_1|I_r(\bar{r})$  is found by replacing  $\epsilon_1$  by  $\frac{\delta r^3}{\rho^3}$ . Visual understanding of this analysis can be gained by considering Figure 5. ++++ contraction in  $I_r$ ?++ The following proposition summarises the the findings for  $\Pi_1$ :

**Proposition 6.5 (?)**

For  $\rho, \delta$  and  $\beta_1$  sufficiently small, the transition map  $\Pi_1 : \Sigma_1^{in} \rightarrow \Sigma_1^{out}$  defined by the flow of system 32 has the following properties:

1.  $\Pi_1(R_1)$  is a wedge-like region in  $\Sigma_1^{out}$ .  $\Pi_1^{-1}(R_2)$  is a wedge-like region in  $\Sigma_1^{in}$ .
2. More precisely, for fixed  $c < 2$ , there exists a constant  $K$  depending on the constants  $c, \rho, \delta$  and  $\beta_1$  such that
  - (a) for  $\bar{\epsilon} \in (0, \delta]$  the map  $\Pi_1|_{I_a(\bar{\epsilon})}$  is a contraction with contraction rate bounded by  $Ke^{-\frac{2c}{3}(\frac{1}{\bar{\epsilon}} - \frac{1}{\delta})}$ .
  - (b) for  $\bar{r} \in (0, \rho]$  the map  $\Pi_1|_{I_r(\bar{r})}$  is a contraction with cocontraction rate bounded by  $Ke^{-\frac{2c}{3}(\frac{\rho^3}{r_1^3\delta} - \frac{1}{\delta})}$ .

## 6.4 Dynamics in $K_3$

Similarly to  $K_1$  and  $K_2$ , the system can be transformed using Equation 22c.

$$\begin{aligned}\frac{dr_3}{dt_3} &= r_3 F(r_3, y_3, \epsilon_3) \\ \frac{dy_3}{dt_3} &= \epsilon_3(r_3 - 1) - 2y_3 F(r_3, y_3, \epsilon_3) \\ \frac{d\epsilon_3}{dt_3} &= -3\epsilon_3 F(r_3, y_3, \epsilon_3)\end{aligned}$$

where  $F(r_3, y_3, \epsilon_3) = (1 - y_3 - \frac{r_3}{3})$

Now if we combine the above three Sections 6.2-6.4, we have now modelled the flow across all of the points in the Van der Pol system, including at our non-hyperbolic fold point. As a result Figure 1 describes the nature



(a) The flow on the Van der Pol for a small  $\epsilon$ .

(b) The flow on the Van der Pol for a larger  $\epsilon$ .

Figure 6: Flow on the Van der Pol system.

in which our trajectories flow across the system where we can see a jump at the fold point, as we deduced from our charts. This now can be extended to a Canard Point, which we will move onto next.

## 7 Canard Points

During this section we will be considering a canard point. This is when our fold point is shifted along the manifold - Figure 7. To adequately explain the effect that the canard point will have on our system we will need

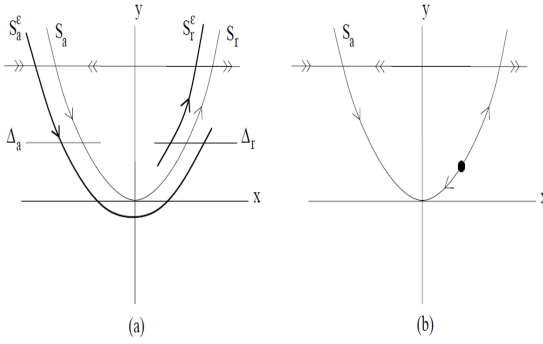


Figure 7: The reduced flow of our system for a)  $\lambda = 0$  and b)  $\lambda > 0$ .

to consider our system,

$$\begin{aligned} x' &= -y + x^2 - \frac{x^3}{3}, \\ y' &= \epsilon(x - 1), \\ \epsilon' &= 0. \end{aligned} \tag{13}$$

Now we need to consider Equation 13 in terms of our canard system. To do this we rewrite our system with an extra parameter  $\lambda$ , where  $\lambda$  is our perturbation of our fold point (?). ? discusses generally how we should continue with computing our canard system. If we apply his theory to the Van der Pol system we find,

$$\begin{aligned} x' &= -y + x^2 - \frac{x^3}{3}, \\ y' &= \epsilon(x - \lambda), \\ \epsilon' &= 0, \\ \lambda' &= 0, \end{aligned} \tag{39}$$

where the change in  $\epsilon$  and  $\lambda$  are constant. Now, for the remainder of the section, we follow the method of ? for the canard system. If we start by rewriting our canard system into the canonical forms we find,

$$x' = -yh_1(x, y, \epsilon, \lambda) + x^2h_2(x, y, \epsilon, \lambda), \tag{40a}$$

$$y' = \epsilon(xh_4(x, y, \epsilon, \lambda) - \lambda h_6(x, y, \epsilon, \lambda)), \tag{40b}$$

Where we note that  $h_j(x, y, \epsilon, \lambda) = 1 + O(x, y, \epsilon, \lambda)$  for  $j = 1, 2, 4, 5$  and  $h_3(x, y, \epsilon, \lambda) = O(x, y, \epsilon, \lambda)$ . However, we should note that for the Van der Pol system our only term that is not solely of leading order is  $h_2(x, y, \epsilon, \lambda) = 1 - \frac{x^3}{3}$ . Now we are able to choose such a  $\lambda > 0$  that produces an equilibrium on our repelling branch  $S_r$  for the reduced flow. By doing this we are then able to define the following conditions for our reduced flow on  $h_j$ ,

$$a_3 = \frac{\partial}{\partial x} h_2(0, 0, 0, 0) = -\frac{1}{3}, \tag{41}$$

$$A = -a_2 + 3a_3 - (2a_4 + 2a_5) = -1, \tag{42}$$

where we notice that our other solutions for  $a_i = 0$  for  $i = 1, 2, 4, 5$  are trivial. The reason that we consider the constant  $A$  is because we will find that this constant is crucial in our canard point analysis iff  $A \neq 0$  (?). Following this (?) discusses the existence of a critical value for  $\lambda$  (denoted  $\lambda_c$ ), where our two branches  $S_r$  and

$S_a$  must connect in a smooth fashion. Now from *Theorem 3.1* we know that we must have a transition map at our critical point,

$$\lambda_c(\sqrt{\epsilon}) = -\epsilon \left( \frac{a_1 + a_5}{2} + \frac{A}{8} \right) + O(\epsilon^{\frac{3}{2}}), \quad (43)$$

which can be written as  $\lambda_c(\sqrt{\epsilon}) = \frac{\epsilon}{8} + O(\epsilon^{\frac{3}{2}})$  for the Van der Pol system (?). Consider Canard cycles and center manifolds / Freddy Dumortier, Robert Roussarie. for more details on canards in Van der Pol .

## 7.1 Canard Blow-up

Now similarly to Section 6 we consider various transformations of our coordinate system to be able to be able to consider the non-hyperbolic equilibrium induced by our canard point. However, as we would expect with our new system we should consider a new set of transformations (?).

$$x = \bar{r}\bar{x}, \quad y = \bar{r}^2y, \quad \epsilon = \bar{r}^2\bar{\epsilon}, \quad \lambda = \bar{r}\bar{\lambda} \quad (44)$$

Now that we have established the transformation we can then define our transformations for  $K_1$  and  $K_2$  but it is not necessary to consider the third chart ( $K_3$ ). This is because we find that the attracting slow manifold connects to the repelling slow manifold. As a result of this we find that our flow will ‘bend back’ from  $K_2$  into  $K_1$  instead of flowing out into the fast flow, which is described by  $K_3$ . This concept can be described by the Figure 8,

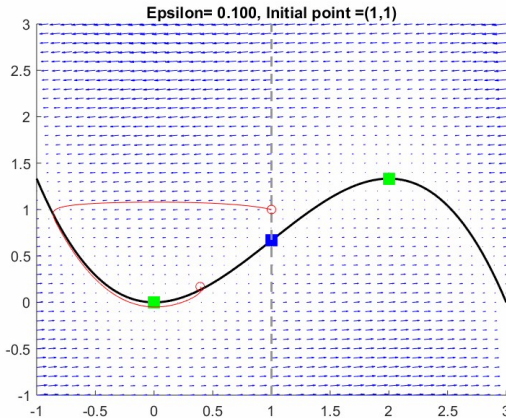


Figure 8: The Van der Pol system for the canard case.

where we can clearly see that our flow need not enter chart  $K_3$  as it ‘bends back’ on itself in the chart  $K_2$  - see Section 1 for a discussion on why  $\epsilon \neq 0$ . Since we have established why we need only consider two charts we can our transformations,

$$x = r_1 x_1, \quad y = r_1^2, \quad \epsilon = r_1^2 \epsilon_1, \quad \lambda = r_1 \lambda_1 \quad (45a)$$

$$x = r_2 x_2, \quad y = r_2^2 y_2, \quad \epsilon = r_2^2, \quad \lambda = r_2 \lambda_2 \quad (45b)$$

Since these transformations have been defined we should consider our charts. We will first consider chart 2, for analogous reasoning to Section ??.

### 7.1.1 Dynamics in $K_2$

We start by noting that we are considering our invariant plane at  $r_2 = 0$  which will significantly simplify our system for  $K_2$ . Further we should note that we are taking a transformation in time,  $\frac{dr}{dt_2} = \frac{dt}{dt_2} \frac{dr}{dt} = \frac{1}{r_2} \frac{dr_2}{dt}$ , as well as in our coordinates. Then if we substitute our time transformation and Equation 45b into our system of Equations 39 we find,

$$\begin{aligned} r_2^2 x'_2 - r_2 x_2 r'_2 &= -r_2^2 y_2 h_1 + r_2^2 x_2^2 h_2, \\ \implies x'_2 &= -y_2 + x_2^2 - r_2 G_2(x_2, y_2), \end{aligned} \quad (46a)$$

$$\begin{aligned} r_2^3 y'_2 - 3r_2^2 y_2 r'_2 &= r_2^2 (r_2 x_2 h_4 - r_2 \lambda_2 h_5), \\ \implies y'_2 &= x_2 - \lambda_2 + r_2 G_2(x_2, y_2), \end{aligned} \quad (46b)$$

where we note that  $h_j = h_j(x, y, \epsilon, \lambda)$  for  $j = 1, 2, 3, 4, 5$ . We should also recall that  $r'_2 = \lambda'_2 = 0$ . Notice that we have included an additional term in Equation 46b - we define  $G_2(x_2, y_2)$  in the following way,  $G(x_2, y_2) = (G_1(x_2, y_2), G_2(x_2, y_2))^T = (-\frac{x_2^2}{3}, 0)^T$ . The reason we also define this vector is to aide in the Melnikov computations which we will see later. ? discusses that for this chart we have an interesting result. They note that at  $r_2 = \lambda_2 = 0$  our system is integrable which allows us to define a constant of motion  $H(x_2, y_2) = \frac{1}{2} \exp(-2y_2) (y_2 - x_2^2 + \frac{1}{2})$  which we can easily verify (?) using the following equations,

$$x'_2 = e^{2y_2} \frac{\partial H}{\partial y_2}(x_2, y_2),$$

$$y'_2 = -e^{2y_2} \frac{\partial H}{\partial x_2}(x_2, y_2).$$

Further to this we can see, when we consider our reduced system, that we have an equilibrium at the origin, implying that  $H(x_2, y_2) = h$ . considering the reduced system (Equation 46) we find from  $H(x_2, y_2) = 0$  that,

$$x'_2 = \frac{1}{2} \implies x_2 = \frac{t_2}{2} + A, \quad (47a)$$

$$y'_2 = \frac{t_2}{2} \implies y_2 = \frac{t_2^2}{4} - \frac{1}{2}, \quad (47b)$$

where we have directly integrated Equation 47a with respect to our time ( $t_2$ ). However, we can note that we are able to choose  $A = 0$  as we are considering an autonomous (time-invariant) system. Then for Equation 47b we are able to rearrange constant of motion at zero to give,  $y_2 = x_2^2 - \frac{1}{2}$ . Clearly from this analysis we are then able to define our trajectories in terms of  $\gamma_{c,2}$ ,

$$\gamma_{c,2}(t_2) = (x_{c,2}(t_2), y_{c,2}(t_2)) = \left( \frac{t_2}{2}, \frac{t_2^2}{4} - \frac{1}{2} \right). \quad (48)$$

Now that we have established that we must have a flow on our second chart, then there must also exist transition maps. Therefore this now enables us to consider the first chart in the following section.

## 7.2 Dynamics in $K_1$

For  $K_1$  we follow a similar approach to the above. We will use the transformations,

$$x = r_1 x_1, \quad y = r_1^2, \quad \epsilon = r_1^2 \epsilon_1, \quad \lambda = r_1 \lambda_1, \quad (45a)$$

to find the relevant pathways of our flows. Now if we first consider the  $r_1$  component,

$$2r_1^2 r'_1 = r_1^2 (r_1 x_1 - r_1 \lambda_1), \quad (49)$$

where we can call  $F = F(x, y, \epsilon, \lambda) = x_1 - \lambda_1 + O(r_1(r_1 + \lambda_1))$ . Now we will see the motivation with starting with  $y = r_1$  when we transform our other coordinates. Now if we consider  $x = r_1 x_1$ ,

$$\begin{aligned} r_1 r'_1 x_1 + r_1^2 x'_1 &= -r_1^2 + r_1^2 x_1^2, \\ x'_1 &= -1 + x_1^2 - \frac{x_1 r'_1}{r_1}, \end{aligned}$$

where we can use Equation 49 to simplify this further - Equation 50.

$$x'_1 = -1 + x_1^2 - \frac{x_1}{r_1} \left( \frac{r_1 \epsilon_1 F}{2} \right) \quad (50)$$

We now consider our  $\epsilon = \epsilon_1 r_1^2$  and noting  $\epsilon' = 0$ . Then we have,  $r_1^3 \epsilon' = -2r_1^2 \epsilon_1 r'_1$ , where we can use Equation 49 to simplify to,

$$\epsilon' = -\epsilon_1^2 F. \quad (51)$$

Our last transformation is for our new coordinate  $\lambda = r_1 \lambda$ , noting that  $\lambda' = 0$ . Similarly to the above we find  $r_1^2 \lambda'_1 + r_1 \lambda_1 r'_1 = 0$  then,

$$\lambda'_1 = -\frac{\lambda_1 \epsilon_1 F}{2}, \quad (52)$$

which is a trivial rearrangement as seen in Equation 51. Now if we combine the above we find that our transformed system is of the following form,

$$r'_1 = \frac{\epsilon}{2} (r_1 x_1 - r_1 \lambda_1), \quad (53a)$$

$$x'_1 = -1 + x_1^2 - \frac{x_1 \epsilon_1 F}{2}, \quad (53b)$$

$$\epsilon' = -\epsilon_1^2 F, \quad (53c)$$

$$\lambda'_1 = -\frac{\lambda_1 \epsilon_1 F}{2}. \quad (53d)$$

From this system we are now able to make some deductions. We first can observe that the hyperplanes are along the  $r_1 = \epsilon_1 = \lambda_1 = 0$  with an invariant line at  $l_1 = \{(x_1, 0, 0, 0) : x_1 \in \mathfrak{N}\}$  (?). As ? discusses the equilibria present at the end of both of our branches - Figure 7 - which are found at  $p_a = (-1, 0, 0, 0)$  and  $p_r = (1, 0, 0, 0)$  (?). Now we can go one step further, we can consider Equation 53 and find the eigenvalues of the system for the invariant planes. We find that,

$$J - \lambda I = \begin{bmatrix} 2x - \lambda & 0 & 0 & 0 \\ 0 & -\lambda & 0 & 0 \\ 0 & 0 & -\lambda & 0 \\ 0 & 0 & 0 & -\lambda \end{bmatrix}, \quad (54)$$

which clearly has three zero eigenvalues and one non-zero eigenvalue  $\lambda = \pm 2$ . Which further emphasises that our equilibrium point is non-hyperbolic. As a result we intuitively expect that something interesting occurs at this point. In the section following we will be considering what effect these mappings and eigenvalues will have on our system.

### 7.2.1 Separation of the Manifolds

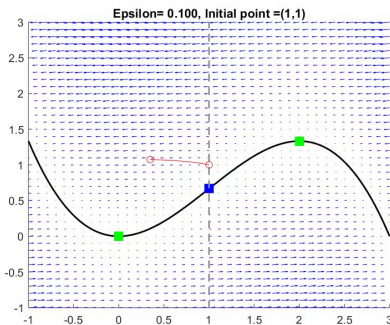
Discuss splitting on the manifold

## 7.3 Effect of the Canard Point

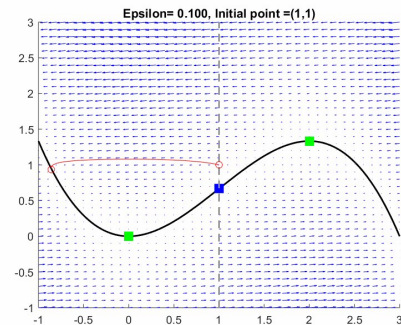
Now that we have shown that there must exist a flow around our fold point we should now consider the global effect of the canard point. We can see by considering the system of Equations 53 that our equilibriums are at  $(x, y) = (\lambda, \lambda^2[\frac{1-\lambda}{3}])$  and find the eigenvalues from the matrix,

$$A - \mu I = \begin{bmatrix} 2x - x^2 - \mu & -1 & 0 & 0 \\ \epsilon & -\mu & x - \lambda & -\epsilon \\ 0 & 0 & -\mu & 0 \\ 0 & 0 & 0 & -\mu \end{bmatrix} = \mu^2(\mu^2 + \mu(x^2 - 2x) + \epsilon). \quad (55)$$

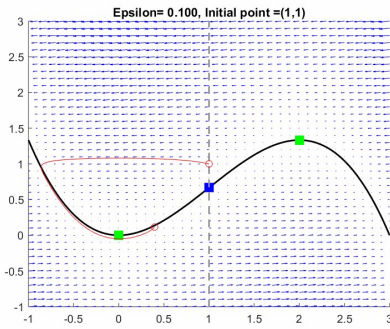
From this we are about to find the eigenvalues of the system,  $\mu = 0$  and  $\mu = \frac{2x-x^2 \pm \sqrt{(x^2-2x)^2-4\epsilon}}{2}$ . Then we consider the values at our equilibrium,  $x = \lambda$ , to find that we have a Hopf Bifurcation when  $4\epsilon > (x^2 - 2x)^2$  or when  $\lambda = 2$  or  $0$ . This then leads to the following trajectories within the flow - Figure 9.



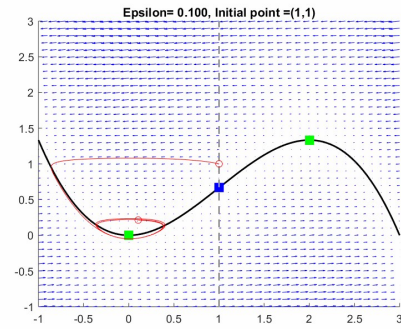
(a) The initial flow within the system.



(b) The flow as it hits the slow manifold.



(c) The flow as it intersects with the fold point.



(d) The Hopf bifurcation due to the canard point.

Figure 9: The trajectories associated with the canards case of the Van der Pol system.

From Figure 9 we can see the progression of our flow over the system. From Figure 9a we see that the flow starts at an initial condition of  $(x, y) = (1, 1)$  and travels along the fast flow towards the attracting branch. Then

from Figure 9b the flow has hit the attracting branch, where it then follows along the slow flow towards the fold point at  $(x, y) = (0, 0)$ , which is described by Figure 9c. Then from Figures 9c and 9d we can observe the Hopf bifurcation. This is because we make note that the canard point is present at  $-\lambda$ , which in essence pushes the flow up the repelling branch (see Figure 7) until the flow is sufficiently far from the fold point where it will then repel towards the attracting branch, starting the oscillation - Figure 9d. Moreover, it is worth noting that our Hopf bifurcation only exists when we are in an arbitrarily small region,  $O(\epsilon)$  ? - this idea is further discussed in Section 7.3.1.

### 7.3.1 Singular Hopf Bifurcation

Furthermore, in the Van der Pol we are able to find a singular Hopf Bifurcation when  $\lambda = 1$ . Then to model this behaviour we need to consider a small perturbation along the slow flow where we will have, from Equation 39,

$$\dot{y} = \lambda - x + \bar{\nu}y, \quad (56)$$

where  $\nu$  is of order  $O(\epsilon)$ , thus small. We can immediately see that when  $\bar{\nu} = 0$  that we have our original flow at our equilibrium but we are now able to perturb our flow over a small domain, which are described in Figures ???. We can also see how our system behaves when our  $\nu$  is of larger order than  $O(\epsilon)$ ,

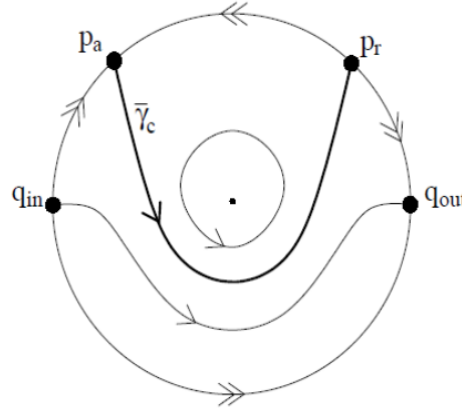


Figure 10: The flow within our canard system (?).

where it is clear that our Hopf bifurcation is the periodic solution in the centre of Figure 10 but we can see that below our special flow  $\bar{\gamma}_c$ , our solution traverses through our equilibrium into our fast flow as we would expect in our original system.

## 8 Folded Singularities in a Three Dimensional System

Now that we have considered the two dimensional case for a folded singularity we can extend it to a third dimension in our system. This can be done by considering a system of one fast and two slow variables such that

$$\begin{cases} \epsilon \dot{x} &= f(x, y, z, y, \epsilon), \\ \dot{y} &= g_1(x, y, z, y, \epsilon), \\ \dot{z} &= g_2(x, y, z, y, \epsilon), \end{cases} \quad (57)$$

which we can see is an extension of our original form - Equation 2 (?). Furthermore, ? also discusses that the addition of an extra slow variable causes issues with respect to the existence of a canard solution. This is because our existence ranges increases from  $O(\epsilon)$  to  $O(1)$ , noting that  $\epsilon \ll 1$  (?). Then for this system we are able to make similar assumptions to the previous case, Section 4, but it is obvious we now must have more than one fold point. We can see that this is the case in Figure 11,

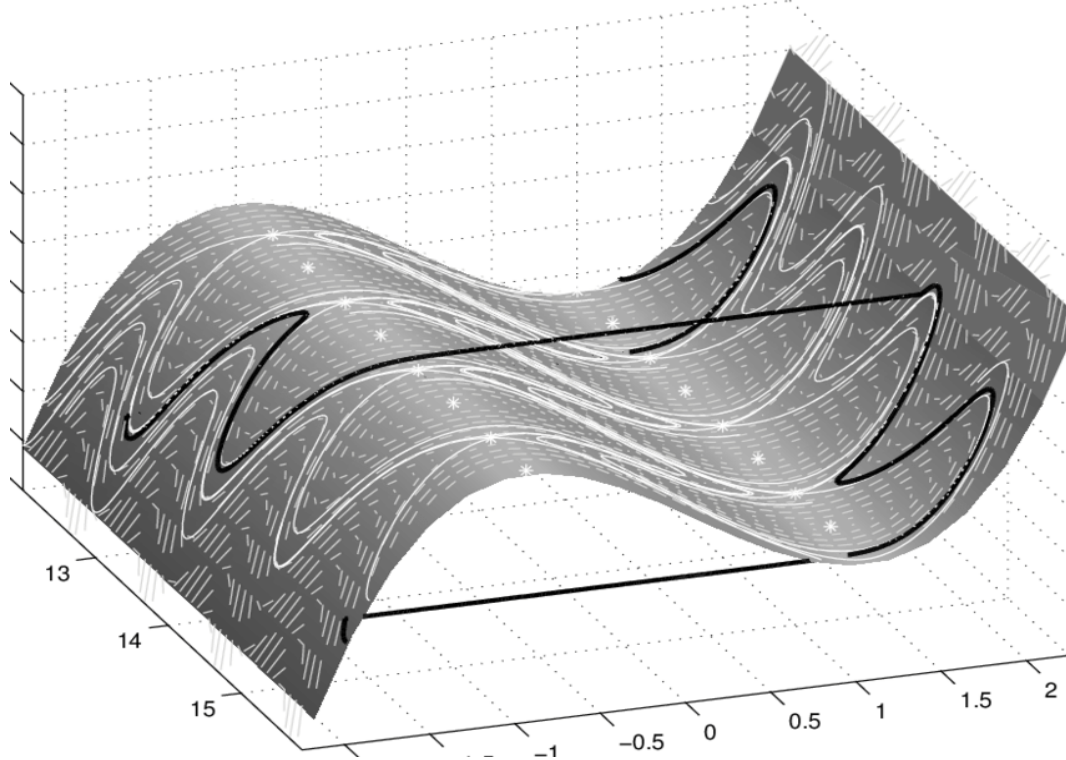


Figure 11: Three dimensional Van der Pol (?).

as our fold point now can take multiple locations within our system, denoted by \*. From here we are able to define some non-degeneracy conditions, much like we did in Section 3,

$$\begin{aligned} f(p_*, \lambda, 0) &= 0, \\ \frac{\partial}{\partial x} f(p_*, \lambda, 0) &= 0, \\ \frac{\partial^2}{\partial x^2} f(p_*, \lambda, 0) &\neq 0, \\ D_{(y,z)} f(p_*, \lambda, 0) &\text{ has full rank one,} \end{aligned} \tag{58}$$

where we denote  $p_* = (x_*, y_*, z_*) \in F$  as our fold points and  $D_{(y,z)} = (\frac{\partial f}{\partial y}, \frac{\partial f}{\partial z})$  are linearly independent of one another (?). In addition to this we can see from Figure 11 that we have some interesting flows within our system. These flows do not follow the standard pattern as we saw in Figure 1, instead the slow flow switches its orientation when the flow hits the fold point and continue to flow in that direction, as a desingularised flow - these are called isolated singularities (?). As a result we are able to express these flows in the following manner, using Equation 58,

$$\begin{cases} \dot{x} = g_1 \frac{\partial f}{\partial y} + g_2 \frac{\partial f}{\partial z} \\ \dot{y} = -g_1 \frac{\partial f}{\partial x}, \\ \dot{z} = -g_2 \frac{\partial f}{\partial x}, \end{cases} \tag{59}$$

where we can then define a folded singularity if  $g_1(p_*, \lambda, 0) \frac{\partial}{\partial y} f(p_*, \lambda, 0) + g_2(p_*, \lambda, 0) \frac{\partial}{\partial z} f(p_*, \lambda, 0) = 0$ , for our flow on branches ( $S$ ) (?). Next we need to consider the stability of our fold points. We do this by constructing the Jacobian of our system,

$$J = \begin{bmatrix} \frac{\partial \dot{x}}{\partial x} & \frac{\partial \dot{x}}{\partial y} & \frac{\partial \dot{x}}{\partial z} \\ \frac{\partial \dot{y}}{\partial x} & \frac{\partial \dot{y}}{\partial y} & \frac{\partial \dot{y}}{\partial z} \\ \frac{\partial \dot{z}}{\partial x} & \frac{\partial \dot{z}}{\partial y} & \frac{\partial \dot{z}}{\partial z} \end{bmatrix}, \tag{60}$$

which we can easily find the eigenvalues, by taking the determinant. The result of this analysis gives that we have three eigenvalues,  $\sigma_i$  for  $i = 1, 2, 3$  (?). Without loss of generality we can choose  $\sigma_3 = 0$  because we know that at least one of our eigenvalues must be zero to account for our fold point in our system - see the Poincaré diagram for further intuition. Then we know from standard stability theory that, at our folded singularity we will have three types of phase portrait in the form of,

$$\begin{cases} \text{Saddle } \sigma_1 \sigma_2 < 0 : \sigma_i \in \Re, \\ \text{Node } \sigma_1 \sigma_2 > 0 : \sigma_i \in \Re, \\ \text{Focus } \sigma_1 \sigma_2 > 0 : \Im(\sigma_i) \neq 0, \end{cases} \tag{61}$$

where we can note that only our focus will have imaginary parts (?). ? illustrates this in the following Figure,

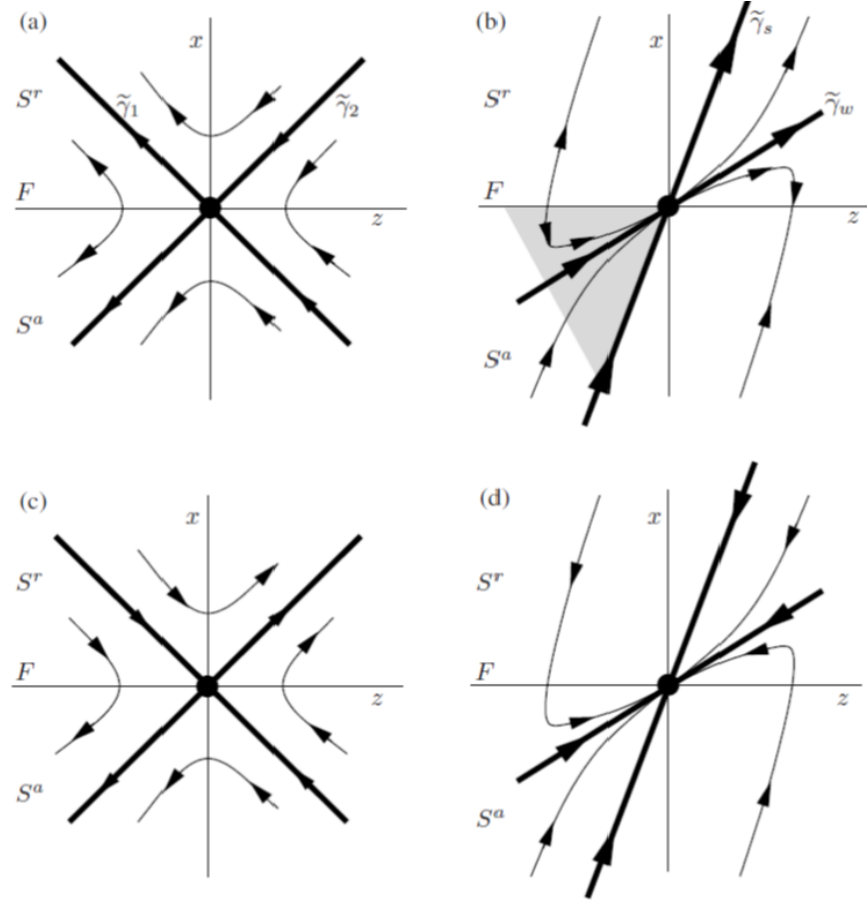


Figure 12: Phase portraits of our three dimensional system where a) is a folded saddle, b) folded node, c) and d) are desingularised flows (?).

where we can see the effect of the varying eigenvalues above. A question which is prudent to consider is, why has not (?) illustrated the singular canard case for a folded focus. This is easily answered as we know that a singular canard is only present if the node or saddle connect our two connecting branches ( $S^r$  and  $S^a$ ). The idea that our branches are connected allows us to note that our flow is able to pass through from an attracting to a repelling manifold, which is described by Figure 12 (?). However, we find that for the focus we are unable to construct branches which connect, preventing the flow from traversing through the fold point. This idea is easily seen as we are able to note, from the imaginary eigenvalues, that there is a spiral present - Figure 13.

Figure 13: The branches of a spiral

It is easily seen, from Figure 13, that it is not possible to construct such a system that allows the flow to traverse this point. We can add further intuition to this example by considering the notion of a source (or sink), which is seen in dynamical systems and fluid mechanics. From a sink (attracting manifold) we know that our flow will always be travelling towards the singularity regardless of its starting location as described by Figure 13 meaning that is impossible to construct a repelling manifold which can connect with this singularity at the fold point - for further information see Figure 14 in Appendix B. where we can see that we are unable to produce a system which has a singular

**Theorem 8.1** (Canards in  $\mathbb{R}^3$  (?)

For slow-fast systems (Equation 57) with  $\epsilon > 0$  sufficiently small the following holds:

- There are no maximal canards generated by a folded focus. For a folded saddle the two singular canards  $\gamma_{1,2}$  perturb to maximal canards  $\gamma_{1,2}$ .
- For a folded node let  $\mu = \frac{\sigma_w}{\sigma_s} < 1$ . the singular canard  $\bar{\gamma}_s$  (“the strong canard”) always perturbs to a maximal canard  $\gamma_s$ . If  $\mu^{-1} \notin \mathbb{N}$ , then the singular canard  $\bar{\gamma}_w$  (“weak canard”) also perturbs to a maximal canard. We call  $\gamma_s$  and  $\gamma_w$  primary canards.
- For a folded node suppose  $k > 0$  is an integer such that  $2k+1 < \mu^{-1} < 2k+3$  and  $\mu^{-1} \neq 2(k+1)$ . Then, in addition to  $\gamma_{s,w}$  there are  $k$  other maximal canards, which we call secondary canard.
- The primary weak canard of a node undergoes a transcritical bifurcation for odd  $\mu^{-1} \in \mathbb{N}$  and a pitchfork bifurcation for even  $\mu^{-1} \in \mathbb{N}$

From Theorem 8.1 we have now defined the existence of a strong and weak eigenvalue such that  $|\sigma_1| > |\sigma_2| \iff |\sigma_s| > |\sigma_w|$ . From this theorem we are then able to carry out explicit investigations, as we will see in Section **Not done yet** noting that a focus is a circle or spiral etc.

## 9 MMO

### 9.1 Oscillations

In this section we consider Mixed Mode Oscillations (MMOs) in fast-slow systems.

**Definition 9.1.** Mixed Mode Oscillations +++ working on it... not good yet+++ A mixed mode oscillation is an orbit  $\gamma$ , which traces out small amplitude oscillations (SAOs) as well as large scale oscillations (LAOs). The large and small amplitude oscillations are clearly separated in the time series and their reoccurrence can be periodic. The signature of an MMO is expressed as  $L_1^{s_1} L_2^{s_2} \dots$  expressing that  $L_1$  number of LAOs are followed by  $s_1$  SAOs.

The cases of MMOs considered here are MMOs associated with folded nodes as well as folded saddle-nodes of type 2, that are associated to singular hopf bifurcations. +++++++needs better intro.++++++

### 9.2 Folded Nodes

### 9.3 Singular Hopf Bifurcation

In this section the folded saddle-node of type 2 and the saddle focus are considered for analysis. The folded saddle-node o type 2 occurs, when the parameters of the system coincide in such a way that an equilibrium of

the full system and a fold point coincide. A saddle-node of type one refers to the case when only an equilibrium of the reduced system crosses a fold, without coinciding with a global equilibrium. If a saddle-node type 2 occurs for a specific parameter (also plural...), then a singular hopf bifurcation arises at  $O(\epsilon)$  away from the equilibrium. The equilibrium is focus if the eigenvalues corresponding to it are complex and a node if the eigenvalues are real.

**Definition 9.2. Singular Hopf Bifurcation[?](but also MMO)**

A singular hopf bifurcation occurs at a certain parameter regime in the system which is  $O(\epsilon)$  away from a saddle-node of type 2. There, the eigenvalues of the system cross the imaginary axis, therefore they have a zero real part. Then small oscillations, called limit cycles occur in the system. There are two types of singular Hopf Bifurcation. The supercritical Hopf Bifurcation occurs when a stable limit cycle arises from an unstable equilibrium point, while the subcritical Hopf Bifurcation causes unstable limit cycles to appear around a stable equilibrium.

These different orbits caused by a singular Hopf Bifurcation are of interest, because they are SAOs of the fast-slow system in question. Therefore, in this chapter we will give an overview of the different SAOs arising from singular Hopf Bifurcations in different parameter regimes. The starting point of the analysis is the normal form considered for the folded node in section +--+toms section+++, which is then modified to a system that displays a singular Hopf Bifurcation and later on a system with a global return mechanism will be derived. The first transformation is achieved by adding higher-order terms to the  $z$  equation of system (++ toms normal form++). It then becomes

$$\begin{aligned}\epsilon \dot{x} &= y - x^2, \\ \dot{y} &= z - x \\ \dot{z} &= -\nu - ax - by - cz,\end{aligned}$$

which is the normal form for a singular Hopf Bifurcation. We then consider a coordinate transformation and time rescaling of the form

$$x = \epsilon^{1/2} \bar{x}, \quad y = \epsilon \bar{y}, \quad z = \epsilon^{1/2} \bar{z}, \quad t = \epsilon^{1/2} \bar{t}.$$

Then the system becomes

$$\bar{x}' = \bar{y} - \bar{x}^2, \tag{62}$$

$$\bar{y}' = \bar{z} - \bar{x}, \tag{63}$$

$$\bar{z}' = -\nu - \epsilon^{1/2} a \bar{x} - \epsilon b \bar{y} - \epsilon^{1/2} c \bar{z}. \tag{64}$$

This transformation can be seen, somewhat equivalently to Section 6.1, as a consideration of a small neighbourhood of the singular point. As described in Section 8, folded singularity is found by examining the critical

manifold  $C = \{(x, y, z) : f := y - x^2 = 0\}$ . The conditions (58) are easily checked and satisfy:

$$\begin{aligned} f(p_*, \nu, \epsilon) &= y - x^2 = 0 \\ \Rightarrow y &= x^2 \\ \frac{\partial}{\partial x} f(p_*, \lambda, 0) &= -2x = 0, \\ \Rightarrow x &= 0 \\ \Rightarrow y &= 0 \\ \frac{\partial^2}{\partial x^2} f(p_*, \lambda, 0) &= -2 \neq 0, \\ D_{(y,z)} f(p_*, \lambda, 0) &= (1, 0) \end{aligned}$$

++++++Help!! Fold conditions do not work out....+ also no idea what the parameters are  $\nu, \epsilon$ ? is it going to zero....++++++ The folded singularity is found at  $p_* = (0, 0, z)$ , which makes the further analysis slightly more straightforward. The equilibria of the system are, such that  $p_0 = (x, x^2, x)$ , where  $x$  satisfies:

$$x = -\frac{1}{2\epsilon^{1/2}b} \left( (a + c) \pm \sqrt{(a + c)^2 - 4b\nu} \right), \quad (65)$$

and therefore there are two equilibria+++is it correct that i have 2??++++ at

$$\begin{aligned} x_1 &= -\frac{a + c}{\epsilon^{1/2}b} + \frac{\nu}{\epsilon^{1/2}(a + c)} + \frac{b\nu^2}{\epsilon^{1/2}(a + c)^3} + \dots \\ x_2 &= \frac{\nu}{\epsilon^{1/2}(a + c)} + \frac{b\nu^2}{\epsilon^{1/2}(a + c)^3} + \dots, \end{aligned}$$

where a MacLaurin expansion for  $\sqrt{(a + c)^2 - 4b\nu}$  has been used. There exists a value for  $x$  depending on the parameters  $a, b, c$  and  $\nu$ , where a fold point intersects with the equilibrium. This is at  $x_1 = 0$  and  $x_2 = 0$ . Then, setting (65) to zero results in

$$\begin{aligned} x &= -\frac{1}{2\epsilon^{1/2}b} \left( (a + c) \pm \sqrt{(a + c)^2 - 4b\nu} \right) = 0 \\ \Rightarrow \nu &= -\frac{(a + c)^2 - (a + c)}{4b}. \end{aligned}$$

Therefore, the location of the singular equilibrium, depends on the parameter values for  $a, b, c$ .

Since  $a, b$  and  $c$  are all multiplied by a factor of  $\epsilon^{1/2}$  or  $\epsilon$  in system (62), we need  $\nu$  to be of  $O(\epsilon^{1/2})$  or smaller in order to observe a singular hopf bifurcation. If  $\nu = O(1)$ , then the factors of  $\epsilon$  in system (62) do not really contribute to the system and are merely a perturbation of the normal form (+++toms normal form+++). If  $\nu \leq O(\epsilon^{1/2})$ , then a singular hopf bifurcation occurs at a distance  $\nu = O(\epsilon)$  in parameter space away from the equilibrium.

Since the eigenvalues of the system are complex, the equilibrium is a saddle-focus, which has not been discussed in the analysis of canard trajectories. (+++loop back to 3dim singularities and why we dont have canards)+++++ The research of the dynamics, and specifically MMOs, close to a singular Hopf Bifurcation is still ongoing. Here we only consider a few specific cases, where  $\nu$  is treated as the main parameter of interest. Furthermore, since the critical manifold in system (62) is in the shape of a quadratic function, by the geometrical nature of the problem, there is no global return mechanism for the system. Trajectories that leave the close proximity of the equilibrium do not return. In order to get MMOs, additionally to the SAOs a global return

mechanism is needed. This is achieved by modifying system (62) by adding a cubic term to the  $x$  equation. This will change the shape of the critical manifold to an S shaped curve and therefore allow for a global return mechanism. The new system is then the following:

$$\begin{aligned}\epsilon \dot{x} &= y - x^2 - x^3, \\ \dot{y} &= z - x, \\ \dot{z} &= -\nu - ax - by - cz.\end{aligned}$$

The expected behaviour of the new system is now to display several SAOs close to the equilibrium, before completing a large amplitude oscillation. This LAO is necessarily of the form of a relaxation oscillation, because there is only one fast variable present in the system. This represents a constraint since the fast subsystem is one dimensional and therefore trajectories are restricted to be monotonic.

## A Elements of Dynamical Systems

In this appendix we state some standard results from dynamical systems theory.

### A.1 Stable Manifold Theorem

Suppose  $\dot{x} = F(x)$  where  $x \in \mathbf{R}^n, F \in C^r(\mathbf{R}^n, \mathbf{R}^n)$  and has only hyperbolic fixed points (i.e. in the associated linearised system  $\dot{x} = Ax, A \in \mathbf{R}^n$  has no eigenvalues  $\lambda$  such that  $\text{Re}(\lambda) = 0$ ).

### A.2 Centre Manifold Theorem

### A.3 Implicit Function Theorem

### A.4 Hartman Grobman Theorem

DO we need this?

### A.5 Hopf Bifurcations

## B Intuitive Examples

### B.1 Folded Focus

For the folded focus, we will consider an approach from fluid mechanics. This is to enable the reader to consider the dynamics within a different field with the aim to give more intuition in a fast-slow dynamical system. To aid with this concept one should consider the motion of water in a bathtub, when the plug has been removed. We can immediately observe that the water will start to spiral around the plug - much like Figure 13 - which acts in a similar fashion to the following figure. From Figure 14 we see that on the left we have a source within

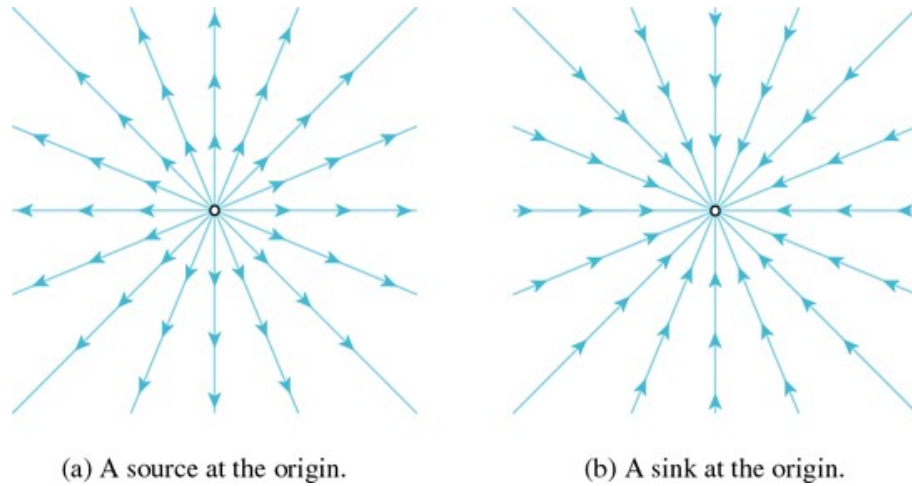


Figure 14: Oversimplified phase plane for a folded focus.

the system, by this we can observe that a source attracts the flow in the system. Whereas on the right we have a sink which can be seen to be repelling the flow, resulting in the jumps (Figure 1) or oscillation in the system - see Sections 4 and 9.1.

## C Numerical Simulation

Many figures in this document? were produced using MATLAB, for example: fig ++++++. In this appendix, we will give a brief tutorial on their production. Fast-slow systems like the ones studied here are a classic example of *stiff* ODEs<sup>a</sup>.

**Definition C.1** (Stiffness Ratio). Consider  $\dot{x} = F(x)$  where  $x \in \mathbf{R}^n, F \in C^r(\mathbf{R}^n, \mathbf{R}^n)$ . Let

$$x' = Ax, \quad A \in \mathbf{R}^{n \times n}$$

denote its linearisation. Suppose all the eigenvalues  $\lambda_j$  of  $A$  have negative real parts. Then the *stiffness ratio*,  $\mu$  is defined as

$$\mu := \frac{\max_j(\operatorname{Re}(\lambda_j))}{\min_j(\operatorname{Re}(\lambda_j))}$$

If  $\mu$  is large, the system is called *stiff*.

Stiffness is not a well-defined concept, it can be seen as a general term for a set of equations which are difficult to solve numerically to a high level of accuracy. Throughout this section we will consider the general problem above as an initial value problem.

$$\begin{cases} \dot{x} = F(x) \\ x(T_0) = x_0 \end{cases}$$

As before,  $x \in \mathbf{R}^n$  and  $F \in C^r(\mathbf{R}^n, \mathbf{R}^n)$ . To solve such a system numerically, time must be discretised. Using standard notation, let  $h$  be the time step between points on the solution. To differentiate between the continuous solution  $x(t)$  and the discretised solution, we denote the latter by  $x(t_j) = x_j$ . Here  $t_j = T_0 + jh$ . As a first example, consider the modified Euler method.

$$x(t_{n+1}) = x(t_n) + hF\left(x(t_n) + \frac{1}{2}F(x(t_n))\right)$$

Or, in the more compact notation,

$$x_{n+1} = x_n + hF\left(x_n + \frac{1}{2}F(x_n)\right)$$

This is a simple method and provides a starting point in considering error between true and numerical solutions.

The go-to ODE solver in MATLAB is `ode45`. This function uses the Dormand-Prince Runge-Kutta method, an explicit single-step formula. The Runge-Kutta method (RK4) is similar to the explicit Euler method in that it calculates the next point ( $x_{n+1}$ ) using only its current value ( $x_n$ ). Unlike the Euler method however, it yields much lower error by using a better approximation of the derivative at points in between  $x_n$  and  $x_{n+1}$  as opposed to only the derivative at the initial point. The Runge-Kutta method uses the following relation.

$$x_{n+1} = x_n + \frac{1}{6}h(k_1 + 2k_2 + 2k_3 + k_4)$$

---

<sup>a</sup>Indeed, the MATLAB documentation for its stiff solver, `ode15s`, uses the Van Der Pol equation as it's example.

where

$$\begin{aligned} k_1 &= F(x_n) \\ k_2 &= F\left(x_n + \frac{1}{2}hk_1\right) \\ k_3 &= F\left(x_n + \frac{1}{2}hk_2\right) \\ k_4 &= F(x_n + hk_3) \end{aligned}$$

The Runge-Kutta family of solvers are ubiquitous in numerical analysis, and most methods can be categorised as belonging to this set of methods. Even the simplest, the explicit Euler scheme, is a RK method.

**Exercise C.2.** Fast slow system example

$$\begin{cases} \dot{x} = -\frac{x}{\epsilon} \\ \dot{y} = -y \end{cases}$$

Test on RK4, mod-Euler and `ode15s?` Intro BDF? Check sec8 MMO.

## D Dynamics in $K_2$